Screening of the Pandemic Response Box identifies anti-microsporidia compounds

Qingyuan Huang[1,2], Jie Chen[1], Guoqing Pan[1#], and Aaron W. Reinke[2#]

[1]State Key Laboratory of Resource Insects, Chongqing Key Laboratory of Microsporidia Infection and Control, Southwest University, Chongqing, China,

[2]Department of Molecular Genetics, University of Toronto, Toronto, ON, Canada

#Corresponding author

gqpan@swu.edu.cn

aaron.reinke@utoronto.ca

Abstract

Microsporidia are fungi-like obligate intracellular pathogens, which infect most animals and cause microsporidiosis. Despite the serious threat that microsporidia pose to humans and agricultural animals, few drugs are available for the treatment and control of microsporidia. To identify novel inhibitors, we took advantage of the model organism *Caenorhabditis elegans* infected with its natural microsporidian *Nematocida parisii*. We used this system to screen the Pandemic Response Box, a collection of 400 diverse compounds with known antimicrobial activity. After testing these compounds in a 96-well format at high (100 μM) and low (40 μM) concentrations, we identified four inhibitors that restored the ability of *C. elegans* to produce progeny in the presence of *N. parisii*. All four compounds reduced the pathogen load of both *N. parisii* and *Pancytospora epiphaga*, a *C. elegans*-infecting microsporidia related to human-infecting species. One of these compounds, a known inhibitor of a viral protease, MMV1006203, inhibited invasion and prevented the firing of spores. An albendazole analog, MMV1782387, inhibited proliferation of *N. parisii*. We tested albendazole as well as 5 other analogs and observed that MMV1782387 was amongst the strongest inhibitors of *N. parisii* and displayed the least host toxicity. Our study further demonstrates the effectiveness of the *C. elegans*-*N. parisii* system for discovering microsporidia inhibitors and the compounds we identified provide potential scaffolds for anti-microsporidia drug development.

Introduction

Microsporidia are obligate intracellular pathogens phylogenetically related to the fungi (Keeling, 2009 , Wadi and Reinke, 2020). Approximately 1700 species of microsporidia have been identified to infect invertebrates, vertebrates, and protists, with at least 17 species infecting human (Chaijarasphong et al., 2021 , Han et al., 2020 , Murareanu et al., 2021). In addition to posing a serious threat to human health, microsporidia are responsible for substantial economic losses in agriculture. Species of farmed penaeid shrimp are susceptible to hepatopancreatic microsporidiosis, which is caused by *Enterocytozoon hepatopenaei* (Chaijarasphong et al., 2021). *Nosema ceranae* and *Nosema apis* are a threat to the global beekeeping industry (Higes et al., 2013 , Forsgren and Fries, 2010). A lethal pathogen, *Nosema bombycis*, causes heavy losses or even total culture failure in the silkworm industry (Bhat et al., 2017). Moreover, some species, such as *Ameson portunus* and *Enterospora nucleophila*, have been identified to infect farmed crabs and fish, respectively (Wang et al., 2017 , Picard-Sánchez et al., 2020). Among immunocompromised individuals, *Enterocytozoon bieneusi* and *Encephalitozoon intestinalis* are the most common microsporidia infections in humans and are associated with diarrhea and systemic illness (Didier, 2005 , Ruan et al., 2021). In underdeveloped countries, up to 51% of HIV-infected individuals with diarrhea have microsporidia infection (Gumbo et al., 1999). Infections with zoonotic microsporidia have been discovered in livestock, companion animals, and wildlife, posing a risk to public health (Widmer et al., 2010). In recent decades, the NIAID and CDC have recognized that many of these species of microsporidia pose a threat to human health. Thus, microsporidia have been classified as Category B priority pathogens for biodefense research (Didier and Khan, 2014).

There are few effective therapeutic interventions available to treat microsporidia infections (Wei et al., 2022). Albendazole is known to inhibit microtubule polymerization by binding beta-tubulin and is effective against a variety of parasites with little adverse effects in humans (Katiyar et al., 1994 , Horton, 2000). In infections of *Encephalitozoon* spp., albendazole has been demonstrated to control microsporidiosis (Li et al., 1996). However, several studies have shown that albendazole has a limited effect on microsporidiosis caused by *E. bieneusi* and *Vittaforma cornea* and that these species encode beta-tubulin with substitutions associated with resistance (Leder et al., 1998 , Franzen et al., 2008 , Akiyoshi et al., 2007). Analogs of albendazole, benomyl and carbendazim, have been used to control microsporidia in insects such as *Nosema heliothidis* in *Heliothis zea* and *Nosema kingi* in *Drosophila willistoni* (Wei et al., 2022 , Armstrong, 1976 , Brooks et al., 1978). However, microsporidiosis in mammals cannot be treated with benomyl and carbendazim because of their hepatotoxicity and toxic effects on reproduction (Sakr et al., 2004 , Barnes et al., 1983) (Kotková et al., 2017). Since benzimidazoles have been widely used for

64 decades, resistance fears have arisen. Fumagillin binds specifically and covalently to methionine
65 aminopeptidase type 2 (MetAP2) and can inhibit many species of microsporidia (Lefkove et al.,
66 2007 , Sin et al., 1997). However, due to concerns with host toxicity, this drug is not approved for
67 use in humans (Han and Weiss, 2018). Furthermore, fumagillin has been associated with
68 concerns regarding its toxicity in agriculture applications (Union, 2010). Therefore, there is a need
69 to identify additional anti-microsporidia inhibiting agents.

70 The model organism *Caenorhabditis elegans* has become a useful system in which to study
71 microsporidia infections and to identify inhibitors. The first microsporidia reported to infect *C.*
72 *elegans* was *Nematocida parisii* (Troemel et al., 2008). Infection of *C. elegans* by *N. parisii* begins
73 when spores are ingested into the worm's intestinal lumen, where they expel their unique invasion
74 apparatus called the polar tube (Tamim El Jarkass and Reinke, 2020). This causes the
75 sporoplasm to be deposited inside intestinal cells. The parasite then proliferates intracellularly as
76 meronts and finally differentiates into spores, which then exit into the intestinal lumen. Infection
77 of *C. elegans* with *N. parisii* results in smaller body size, reduced reproductive fitness, and
78 shortened life span (Balla et al., 2015 , Balla et al., 2016 , Willis et al., 2021). This host-parasite
79 system has become a model in which to study mechanisms of microsporidia invasion, proliferation,
80 and spore exit (El Jarkass et al., 2022 , Reinke et al., 2017 , Balla et al., 2016 , Szumowski et al.,
81 2014). Other species of microsporidia have also been found to infect *C. elegans* including
82 *Pancytospora epiphaga*, which is related to human-infecting species (Bojko et al., 2022 , Wadi et
83 al., 2023 , Zhang et al., 2016). We recently described the use of *C. elegans* to screen compounds
84 for activity towards *N. parisii* using a high-throughput 96-well based assay, resulting in the
85 identification of inhibitors of microsporidia invasion and proliferation (Han et al., 2020 , El Jarkass
86 et al., 2022 , Murareanu et al., 2022).

87 The Pandemic Response Box (PRB) is a promising source of anti-microsporidia compounds.
88 Developed by the Medicines for Malaria Venture with the support of the Drugs for Neglected
89 Disease Initiative, this is an open-access compound library consisting of 400 small molecule
90 compounds that have antifungal, antibacterial and antiviral activity (Samby et al., 2022).
91 Compounds from this collection include those that can inhibit other types of parasites such as
92 nematodes, amoebas, and the causative agent of malaria (Shanley et al., 2022 , Reader et al.,
93 2021 , Rice et al., 2020).

94 To identify novel microsporidia inhibitors, we screened the PRB using a modified version of our
95 previously described *C. elegans-N. parisii* assay (Murareanu et al., 2022). We screened this
96 compound collection at two concentrations and identified four chemical inhibitors of microsporidia

97 infection. We validated these compounds and additionally show that all four compounds reduced
98 the pathogen load of *N. parisii*. We then studied at what stage in the microsporidia life cycle each
99 compound is active. We found that MMV1782387, an analog of albendazole, inhibits
100 microsporidian proliferation. This compound and other albendazole analogs were identified inhibit
101 both *N. parisii* and *P. epiphaga.* We also show that MMV1006203 inhibits spore firing and related
102 flavone analogs also prevent *N. parisii* infection. Together our study identifies additional
103 microsporidia inhibitors that can block microsporidia proliferation and invasion.

104

105 **Results**

106 **Screen of Pandemic Response Box identifies 4 microsporidia inhibitors**

107 To identify compounds from the Pandemic Response Box collection which inhibit microsporidia
108 infection, we adapted our previously described 96-well infection assays (Murareanu et al., 2022).
109 Earliest larval (L1) stage of *C. elegans* were incubated with *N. parisii* spores and compound in
110 liquid for six days at 21°C. Host animals infected with *N. parisii* produce a reduced number of
111 offspring and compounds which inhibit microsporidia can restore the ability of these animals to
112 produce progeny. To quantify the number of offspring produced when incubated with each
113 compound, animals in each well were stained with rose bengal, imaged with a flatbed scanner,
114 and counted using WorMachine (Hakim et al., 2018)(see methods). Each compound was
115 screened in triplicate at a concentration of 100 μM. We identified six compounds that increased
116 progeny production in infected worms by 35-90% relative to the uninfected controls (Fig. 1A).
117 These compounds also increased progeny production by 1.7-8.5-fold compared to infected
118 controls. Four of these compounds significantly improved the production of *C. elegans* progeny
119 in the presence of *N. parisii* (Fig. 1B-D). To determine the effect of the compound collection at a
120 lower concentration, we screened each compound at 40 μM. We observed three compounds
121 which increased progeny production over 3-5.3-fold more than infected controls and to more than
122 13% of the uninfected controls (Fig. 1E). Two of these compounds resulted in significantly more
123 progeny production at 40 μM and these two compounds were also observed to be significant at
124 100 μM (1F and 1G). In total we identified four compounds with significant activity which we
125 validated and characterized in subsequent experiments (Fig. 1H).

126 We next sought to determine whether the four compounds which significantly restored *C. elegans*
127 progeny production also limited *N. parisii* infection. We set up assays similar to our initial screen
128 by culturing L1 worms continuously with *N. parisii* spores in the presence of compounds in 24-

129 well plates. After four days, worms were fixed and then stained with direct yellow 96 (DY96), which
130 binds to chitin, a critical component of *N. parisii* spore walls and *C. elegans* embryos (Fig. 2A)
131 (Zhang et al., 2016 , Vávra and Ronny Larsson, 2014 , Willis et al., 2022). In the presence of *N.*
132 *parisii* spores, all four compounds significantly increased the proportion of adult worms containing
133 embryos (Fig. 2B), which is consistent with the results from our initial screen. Treatment with the
134 newly discovered compounds and the known microsporidia inhibitor dexrazoxane significantly
135 reduced animals displaying newly formed *N. parisii* spores, except for MMV1593539 (Fig. 2C)
136 (Murareanu et al., 2022). To determine if MMV1593539 had any impact on *N. parisii* infection, we
137 quantified the proportion of worms displaying a low, moderate, or high infection level (See
138 methods) (Fig. 2D-F). Under these infection conditions, ~90 percent of control worms displayed
139 high infection levels and all four compounds significantly lowered infection (Fig. 2F).

140

141 **MMV1782387 inhibits the proliferation of *N. parisii***

142 The identified compounds could inhibit microsporidia infection through two mechanisms: by
143 preventing microsporidia from invading cells or by reducing proliferation after invasion. To test
144 whether compounds limited proliferation, we set up pulse-chase experiments where we infected
145 worms for three hours, washed away excess spores, and then incubated the worms with one of
146 the four MMV compounds or with dexrazoxane which was previously shown to limit *N. parisii*
147 proliferation (Fig. 3A) (Murareanu et al., 2022). Treatment with MMV1782387 and dexrazoxane
148 increased the gravidity of worms (Fig. 3B). Treatment with MMV1782387 also inhibited *N. parisii*
149 proliferation with 26.67% of worms having newly formed spores, which is less inhibition than was
150 observed with dexrazoxane (0.89%) (Fig. 3C).

151 To determine whether MMV1782387 inhibits *N. parisii* by slowing proliferation or enhancing
152 parasite clearance, we examined pulse-chase infected animals at either 2 day (before spore
153 formation) or 4 days (after spore formation) post infection with probes specific for *N. parisii* 18S
154 RNA (Troemel et al., 2008). Dexrazoxane was previously shown to significantly reduce the
155 pathogen burden within animals, without influencing the proportion of infected animals
156 (Murareanu et al., 2022). We observed that MMV1782387, similar to dexrazoxane, did not cause
157 a reduction in infected animals, but significantly reduced the amount of meronts in the worms (Fig.
158 3D-3F). None of the other MMV compounds we tested reduced pathogen load of the worms at
159 either 2- or 4-days post-treatment. Dexrazoxane also caused significantly more reduction in

160 pathogen levels compared to MMV1782387 (Fig. 3E and 3F). Together our results show
161 MMV1782387 inhibits microsporidia proliferation but does not enhance parasite clearance.

162

163 **Spore firing is inhibited by MMV1006203**

164 The initial step of microsporidia invasion is spore germination. Many microsporidia, including *N.*
165 *parisii*, germinate (also called spore firing) in the intestinal lumen to initiate infection (Fries et al.,
166 1996 , Troemel et al., 2008 , Lv et al., 2022). In order to determine whether any compounds
167 reduce germination, we conducted spore firing assays using the four MMV compounds as well as
168 ZPCK, which has previously been shown to inhibit spore germination (Murareanu et al., 2022). *N.*
169 *parisii* spores were incubated with compounds for 24 hours and the spores were then washed to
170 remove the compounds. These spores were then cultured with *C. elegans* at the L1 stage for
171 three hours and stained with FISH to visualize the sporoplasms and DY96 to visualize the spores.
172 Spore firing was determined by counting the number of spores that did not contain a sporoplasm
173 divided by the total number of spores. ZPCK and one of the MMV compound, MMV1006203,
174 significantly reduced the spore firing rate (Fig. 4A). All of the compounds, as well as ZPCK, also
175 significantly reduced the number of sporoplasms that had invaded each worm (Fig. 4B).

176

177 **Benzimidazole and flavone analogs inhibit *N. parisii* infection**

178 The benzimidazole molecule albendazole is one of the main treatment options currently used for
179 microsporidia infection. The structure of MMV1782387 is similar to albendazole and the PRB
180 contains several other benzimidazoles including carbendazim, fenbendazole, and oxfendazole.
181 However, these other benzimidazole compounds were not identified in our initial screen. We first
182 tested whether MMV1782387 and six benzimidazole analogs reduced the reproductive fitness of
183 uninfected *C. elegans* (Fig. 5G). At 40 μM, there is no difference in the percentage of worms
184 forming embryos when treated with any of the compounds (Fig. 5A). In contrast, menbendazole
185 and oxfenfazole significantly reduced progeny production in uninfected animals at 100 μM,
186 indicating moderate toxicity to the host (Fig. 5D). We then tested whether these benzimidazole
187 compounds could restore the formation of embryos in animals infected with *N. parisii* using our
188 continuous infection assays. Except thiabendazole, all of the compounds increased the
189 percentage of gravid worms in the presence of *N. parisii* at 40 μM (Fig. 5B). At 100 μM,
190 MMV1782387, albendazole, and carbendazim increased the percentage of gravid worms with *N.*

191 *parisii* (Fig. E). MMV1782387-treated worms displayed the largest increase in the percentage of
192 gravid worms. We also examined the percentage of worms with newly formed spores when
193 treated with these compounds. Except thiabendazole, all compounds displayed a reduction in
194 infected animals at 40 μM (Fig. 5C). All compounds displayed a reduction in infected animals at
195 100 μM, with MMV1782387 displaying amongst the strongest inhibition of infection (Fig. 5F).
196 These results suggest that benzimidazoles can inhibit *N. parisii* and that MMV1782387 shows
197 both strong inhibition of *N. parisii* as well as low host toxicity in *C. elegans*.

198 The compound we identified which inhibits spore firing, MMV1006203, has a structure similar to
199 flavone. To test whether flavone and an analog of MMV1006203, displurigen, could inhibit *N.*
200 *parisii*, we tested these compounds in continuous infection assays at a concentration of 40 μM or
201 100 μM (Fig. 5L). All three of these compounds significantly increased the proportion of gravid
202 worms and reduced infection rates at a concentration of 40 μM (Fig. 5H and 5I). At a concentration
203 of 100 μM, all three molecules were effective at inhibiting microsporidia infection, though only
204 MMV1006203 could significantly increase the gravidity of worms (Fig. 5J and 5K). These results
205 show that molecules based on a flavone structure can inhibit *N. parisii* infection.

206

207 **Identified MMV compounds inhibit *P. epiphaga***

208 To test whether the four MMV compounds we identified were effective against other microsporidia
209 species, we tested them against *P. epiphaga.* This species of microsporidia infects the
210 hypodermis and muscle of *C. elegans* and belongs to the *Enterocytozoonida* clade, along with
211 the human pathogens *V. cornea* and *E. bieneusi* (Zhang et al., 2016 , Bojko et al., 2022). In order
212 to examine whether the four inhibitors we identified from the PRB could inhibit *P. epiphaga*
213 infection of *C. elegans*, we used FISH staining to quantify the pathogen load. All of the compounds
214 significantly reduced *P. epiphaga* infection levels (Fig. 6A). *V. cornea* and *E. bieneusi* contain a
215 glutamine at position 198 in beta-tubulin that is associated with albendazole resistance, but *P.*
216 *epiphaga* beta-tubulin encodes for glutamate at this position which is associated with albendazole
217 sensitivity (Franzen et al., 2008 , Akiyoshi et al., 2007 , Wadi et al., 2023). We tested albendazole
218 against *P. epiphaga* and observed that this compound also inhibited infection (Fig. 6B).

219

220 **Discussion**

221 We screened the open-access PRB compound library, identifying four compounds with anti-
222 microsporidia activity. We quantified the ability of compounds to reproducibly alleviate the
223 reduction in *C. elegans* progeny caused by *N. parisii* infection. We validated all four compounds
224 identified from the initial screen, which is an improvement over our previous screen where we
225 qualitatively determined the effect of compounds from a single replicate and only about half of the
226 initially identified compounds were validated (Murareanu et al., 2022). All four compounds we
227 identified in this study limited both *N. parisii* and *P. epiphaga* infection. These results further
228 demonstrate that *C. elegans* can be used to efficiently identify compounds with activity against
229 multiple species of microsporidia. One limitation of our approach is that inhibitors that reduce the
230 reproductive fitness of *C. elegans* on their own will not be observed. However, this is also
231 potentially beneficial as host toxicity, at least within the *C. elegans* context, is evaluated at the
232 same time as inhibition of microsporidia infection.

233 There is a range of bioactivity associated with benzimidazoles, including anti-inflammatory,
234 antihypertensive, anti-bacterial, anti-parasitic, and anti-fungal properties (Labanauskas et al.,
235 2004 , Navarrete-Vázquez et al., 2010 , Hosamani and Shingalapur, 2011 , Wei et al., 2022). The
236 benzimidazole albendazole is one of the most common treatments for microsporidia. Here we
237 show that MMV1782387, a benzimidazole carbamate, has amongst the strongest inhibition of *N.*
238 *parisii* and relatively low host toxicity in *C. elegans*. Carbendazim, fenbendazole and oxfendazole
239 are present in the PRB, however, in our preliminary screening, we did not find that these
240 compounds improved progeny production in the presence of *N. parisii*. Beta-tubulin is the likely
241 target of albendazole in microsporidia, and given the similarity of the compounds, MMV1782387
242 may also inhibit beta-tubulin. In compound library screens, multistage activity is one of the most
243 preferred attributes for antipathogens (Poonam et al., 2018). We show that MMV1782387, which
244 inhibits proliferation of *N. parisii* can also reduce invasion by about 50%. MMV1782387 has been
245 shown to be effective against several fungal pathogens which cause eumycetoma and may have
246 potential for further development as an inhibitor of fungal pathogens (Lim et al., 2022).

247 Microsporidia infect host cells through spore germination, and this process may be regulated by
248 receptor proteins on cell membranes and external signals (Undeen, 1990 , Willis and Reinke,
249 2022). Furthermore, the changes in calcium ion concentrations, osmotic pressure of the external
250 medium, or *in vivo* host environments can induce microsporidia spore firing (Weidner and Byrd,
251 1982 , Pleshinger and Weidner, 1985 , UNDEEN and FRIXIONE, 1990). However, many of the
252 microsporidia proteins involved in spore firing are unknown. The subtilisin-like protease NbSLP1
253 has been implicated in germination as the active version localizes to the site of the spore where

254 polar tube firing occurs in *N. bombycis* spores (Dang et al., 2013) (Wang et al., 2022). We
255 previously found that protease inhibitors and quinones can inhibit spore firing (Murareanu et al.,
256 2022). Here we show that MMV1006203, a flavone, can prevent microsporidia invasion and spore
257 firing. This inhibition occurs after incubation of the compound with spores, followed by washing of
258 the spores, suggesting that this inhibitor acts directly on the spores to prevent firing. The molecular
259 structures of displurigen and flavone are similar to that of MMV1006203, and these compounds
260 also display the ability to prevent *N. parisii* infection. Other flavone compounds such as quercetin
261 were shown to inhibit *Encephalitozoon intestinalis* infection, but it was not determined if these
262 compounds block microsporidia invasion (Mead and McNair, 2006). MMV1006203 was first
263 shown to inhibit the human cytomegalovirus (HCMV) protease and more recently to have activity
264 against *Plasmodium falciparum* (Reader et al., 2021 , Dhanak et al., 1998). Further work will be
265 necessary to determine the molecular target of MMV1006203 in preventing microsporidia spore
266 firing.

267

268 **Acknowledgements**

269 We are grateful to Winnie Zhao, Yin Chen Wan, Meng Xiao, Jonathan Tersigni, Hala Tamim El
270 Jarkass, and Edward James for providing helpful comments on the manuscript. We thank the
271 Medicines for Malaria Venture for providing the PRB compound library and the individual
272 compounds to retest. **Funding:** This work was supported by Canadian Institutes of Health
273 Research grant (no. 461807 to A. W. R.) and Q. H was supported by an award from the China
274 Scholarship Council. **Competing interests:** The authors declare that they have no competing
275 interests. **Data availability:** All data is presented in Data S1.

276

277 **Material and Methods**

278 *C. elegans maintenance*

279 The food source for *C. elegans*, *Escherichia coli* OP50-1, was grown to saturation in lysogeny
280 broth (LB) for 18 hours at 37°C. To generate animals for infection assays, the wild-type *C. elegans*
281 strain N2 was grown as a mixed population and L4 stage worms were picked onto a 10 cm
282 nematode growth media (NGM) plates seeded with 10x OP50-1 *E. coli* and kept at 21°C for 4
283 days (Lewis and Fleming, 1995). In order to synchronize the worms, M9 solution was used to
284 remove the worms from the NGM plates, sodium hypochlorite and sodium hydroxide were used

285 to bleach them. Embryos from gravid adults were released into the solution and after washing
286 were incubated at 21°C for 18 to 24 hours until the embryos hatched.

287 *N. parisii spore preparation*

288 *N. parisii* (ERTm1) spores were prepared as described previously (Willis et al., 2021). *C. elegans*
289 N2 worms were infected with *N. parisii* spores on NGM plates. Worms were incubated for several
290 days to generate a large population of infected worms, which were harvested and frozen at -80°C.
291 Zirconia beads (2 mm diameter) were used for mechanical disruption of the infected worms,
292 followed by the removal of embryos, larvae, and debris using a 5 µm filter (Millipore). *N. parisii*
293 spore preparations were confirmed to be free of contaminated bacteria and stored at -80°C. Spore
294 concentration was measured by counting DY96-stained spores using a sperm counting slide
295 (Cell-VU).

296 *Source of chemicals*

297 Medicines for Malaria Venture (MMV, Geneva, Switzerland) provided 400 compounds dissolved
298 in 10 µL of DMSO at a concentration of 10 mM for inclusion in the Pandemic Response Box (PRB).
299 2 µL of the stock compounds were transferred to new plates containing 3 µL DMSO to generate
300 4 mM stocks. For retesting, the individual compounds of MMV1006203, MMV1593539,
301 MMV1634497 and MMV1782387 were a gift from MMV. The analog compounds of albendazole,
302 thiabendazole, carbendazim, oxfendazole, mebendazole, fenbendazole, flavone and displurigen
303 were purchased from MilliporeSigma. Stocks of all compounds were stored at -80 °C.

304 *Phenotypic assays in 96-well plates to identify microsporidia inhibitors*

305 Previously described methods were adapted to quantify the ability of compounds to restore the
306 ability of *C. elegans* to produce progeny in the presence of *N. parisii* (Murareanu et al., 2022).
307 Each well of a 96-well plate was filled with 25 µL of K-medium (51 mM NaCl, 32 mM KCl, 3 mM
308 $CaCl_2$, 3 mM $MgSO_4$, 3.25 µM cholesterol) containing 5x OP-50 and *N. parisii* spores, with the
309 exception of column 12 to which spores were not added. 25 µL of K-medium containing L1 worms
310 was then added to each well. 500 nL of compounds from the PRB were pinned into columns 2–
311 11 using a 96-well pinning tool manufactured by V&P Scientific. Additionally, 500 nL of DMSO
312 was added to columns 1 and 12 for infected and uninfected controls, respectively. Each well
313 contained 100 bleach-synchronized L1 worms, 1% DMSO, 15000 spores/µL *N. parisii* and 100
314 µM or 40 µM of compounds. A breathable adhesive porous film was used to cover the 96-well
315 plates, which were placed inside humidity boxes wrapped in parafilm and incubated for 6 days at

316 21°C with shaking at 180 rpm. Each compound was tested three times at both concentrations,
317 with the exception of 17 compounds for which there was not sufficient amounts at which to test at
318 100 μM and 9 compounds there was not sufficient amounts at which to test at 40 μM (See Data
319 S1).

320 *Quantification of progeny production*

321 Following incubation, 10 μL of 0.3125 mg/mL Rose Bengal solution was added to each well using
322 an Integra VIAFLO 96 Electronic pipette. Plates were then wrapped in parafilm and incubated for
323 16–24 hours at 37 °C, resulting in magenta staining of the worms. 240 μL M9/0.1%Tween 20
324 was added to each well and the plate and centrifuged for 1 minute at 2200 x g. 200 μL supernatant
325 was removed from each well and 150 μL of M9/0.1%Tween 20 was added to each well. Upon
326 mixing up the worms in the plate, 25 μL of the worms were transferred to 96-well white clear
327 bottom plates containing 300 μL M9/0.1%Tween 20. After 30 minutes, plates were scanned using
328 an Epson Perfection V850 Pro flat-bed scanner with the following settings: positive film-holder,
329 4800 dpi, and 24-bit color. In order to highlight stained worms, images were also modified using
330 GIMP version 2.8.18, with horizontal and vertical gridlines positioned such that each well is
331 separated by a grid and removing HTML color codes #000000 and #FFC9AF. Images were also
332 modified by applying unsharp masking with the following parameters (radius = 10, effect = 10,
333 threshold = 10). Hue saturation was adjusted by changing the lightness to 100 and the saturation
334 to -100 for yellow, blue, cyan, and green. For red and magenta, the lightness was changed to -
335 100 and the saturation to 100. Each well was exported as a single .tiff image using LZW
336 compression. MATLAB was used to run WorMachine (Hakim et al., 2018) with the pixel
337 binarization threshold set to 30, the neighboring threshold to set to 1, and the maximum object
338 area set toto 0.003%.

339 *Continuous infection assays*

340 24-well assay plate containing a total volume of 400 μL including800 L1 worms and 15,000 *N.*
341 *parisii* spores/μL were used for continuous infection assays. Assays were performed for three
342 biological replicates using 100 μM of each compound except for dexrazoxane (60 μM). During the
343 incubation period, test plates were covered with breathable adhesive porous film, the boxes were
344 enclosed in parafilm, and the plates were incubated at 21 °C, with shaking at 180 rpm for four
345 days. Incubated samples were washed with M9/0.1%Tween 20, acetone-fixed, DY96-stained,
346 and analyzed by fluorescence microscopy.

347 *Pulse infection assays*

348 To generate infected worms, ~8000 bleach-synchronized L1 worms, 30 million *N. parisii* spores,
349 and 5 µL 10x OP50-1 were added to 6 cm NGM plates and incubated for three hours at 21 °C
350 after drying. To remove excess spores, the worms were washed twice with 5 mL M9/0.1%Tween
351 20. Worms were then added to 24-well plates and set up as described in the continuous infection
352 assays, with the exception that no spores were added. For each of the biological replicates, three
353 wells were assayed for each compound. After incubation for 2 or 4 days as described above,
354 samples were fixed in acetone and stained with DY96 and a FISH probe as described below.

355 *Spore firing assays*

356 Spores at a concentration of 30000 spores/µL were incubated for 24 h at 21 °C with compounds
357 at a concentration of 200 µM, except for ZPCK was at 120 µM, and 2% DMSO. After being washed
358 three times with 1 mL K-medium, the spores were used in the 24-well assay plates as described
359 above. The final concentrations in these assays were 15000 spores/ µL, 100 µM compounds
360 except ZPCK (60 µM), and 1% DMSO. Each compound was tested in three biological replicates
361 in all assays. Incubation was performed as described above and after 3 h, samples were fixed in
362 acetone, stained with FISH and DY96, and examined by fluorescence microscopy.

363 *DY96 staining, fluorescence in situ hybridization (FISH), and fluorescence microscopy*

364 To remove excess OP50, samples were washed twice in 1 mL M9/0.1%Tween 20. They were
365 fixed in 700 µL acetone for 15 minutes or 500 µL PFA solution (4% PFA, 1x PBS, 0.1% Tween-
366 20) for 30 minutes. Then, samples were washed twice in PBS/0.1%Tween 20. For DY96 staining,
367 500 µL DY96 staining solution (10 µg/µL DY96, 0.1% SDS in 1xPBS + 0.1% Tween-20) was
368 added and samples were rotated for 30 minutes. EverBrite™ Mounting Medium with DAPI was
369 then added to the samples. FISH was performed using the microB FISH probe for *N. parisii* 18S
370 rRNA (ctctcggcactccttcctg) conjugated to Cal Fluor Red 610 (LGC Biosearch Technologies)
371 (Troemel et al., 2008). After washing with PBS/0.1%Tween 20, samples were incubated in
372 hybridization buffer (900 mM NaCl, 20 mM pH=8 Tris HCl, 0.01% SDS) containing 5 ng/µL FISH
373 probe at 46 °C for 1-6 hours. Samples were washed once with 1 mL wash buffer (50 mL
374 hybridization buffer + 5 mM EDTA). These samples were also stained with DY96 as described
375 above, except with DY96 at 20 µg/µL. Samples were imaged using a ZEISS Axio Imager 2 at 5x–
376 63x magnification and images were captured using Zeiss Zen 2.3. Gravid worms were defined as
377 the proportion of animals containing any number of embryos. Infected worms were defined as the
378 proportion of animals displaying any newly formed spores. Low infection was defined as spores
379 present in less than one half of an animal, moderate infection was defined as spore present in

380 half of an animal, and high infection was define as spores present throughout both halves of an
381 animal. L1 progeny of the parents could be distinguished in size and were not included in these
382 measurements.

383 *P. epiphaga infection assays*

384 *P. epiphaga* strain JUm1396 spores were prepared similar to as described above for *N. parisii*.
385 For infection experiments with *P. epiphaga*, 24-well assay plates were set up to contain a final
386 volume of 400 µL in K-medium, including 800 L1 worms and 80,000 P. epiphaga spores /µL. All
387 compounds were at a concentration of 100 µM, except for dexrazoxane which was used at 60
388 µM. The final concentration of DMSO was 1%. Plates were incubated as described above for four
389 days. The samples were fixed in 4% PFA and stained by the FISH probe specific to *P. epiphaga*
390 18S RNA (CAL Fluor Red 610CTCTATACTGTGCGCACGG). Fluorescence microscopy and
391 quantification of FISH fluorescence were performed as described above.

392 *Statistical analyses*

393 The data were collected from three independent experiments with 3 biological repetition and
394 analyzed by GraphPad Prism. The two groups were compared using the student's t-tests.
395 Statistical significance was defined as $p<0.05$, $*p<0.01$, $***p<0.001$, and $****p<0.0001$.

396

397 **Figures and legends**

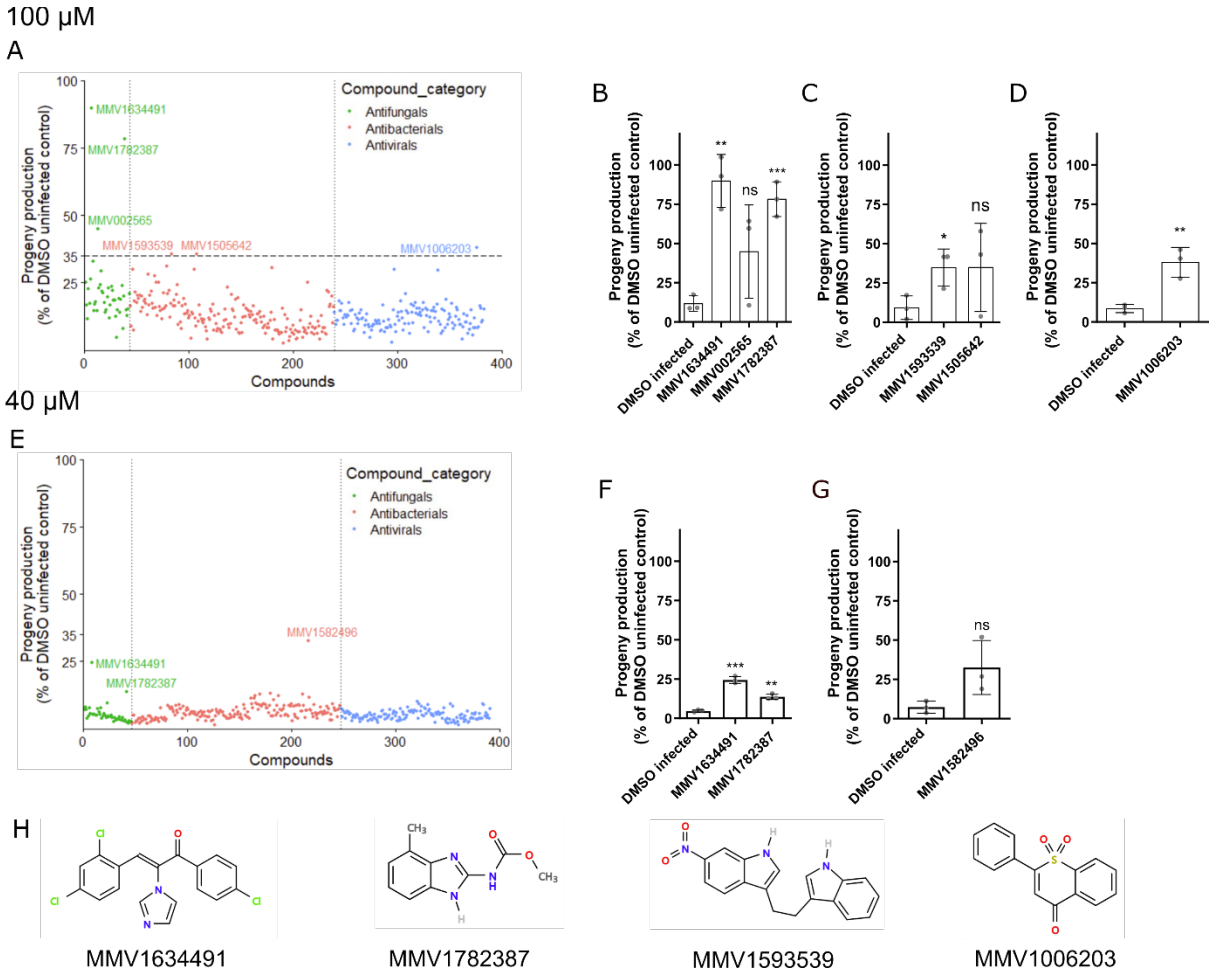

398

Fig. 1. Four compounds from the Pandemic Response Box restored *C. elegans* progeny production in the presence of *N. parisii*. A, E Compounds at concentration of 100 µM (A) or 40 µM (E) were incubated with *C. elegans* and *N. parisii* for 6 days. Each point represents the mean progeny production of a compound expressed as the percentage of the DMSO uninfected control. The compound-ID is shown for compounds that had an activity of at least 35% (A) or ≥ 13% (E). Compounds are divided into their disease area as classified by the PRB and colored according to the legend at the right. 17 compounds in the collection were not screened at 100 µM and 9 compounds not screened at 40 µM due to lack of material (Data S1). **B-D** Compounds that had an activity of at least 35% at 100 µM. (B) Antifungals, (C) Antibacterials, (D) Antivirals. **F,G** Compounds that had an activity ≥ 13% at 40 µM. (F) Antifungals, (G) Antibacterials. **H** The chemical structures of the four PRB compounds with significant activity. Statistical significance was determined by Student's t-test with comparisons to the DMSO infected control Means ± SD (horizontal bars) are shown. (*$p < 0.05$, **$p < 0.01$, ***$p < 0.001$, ns means not significant).

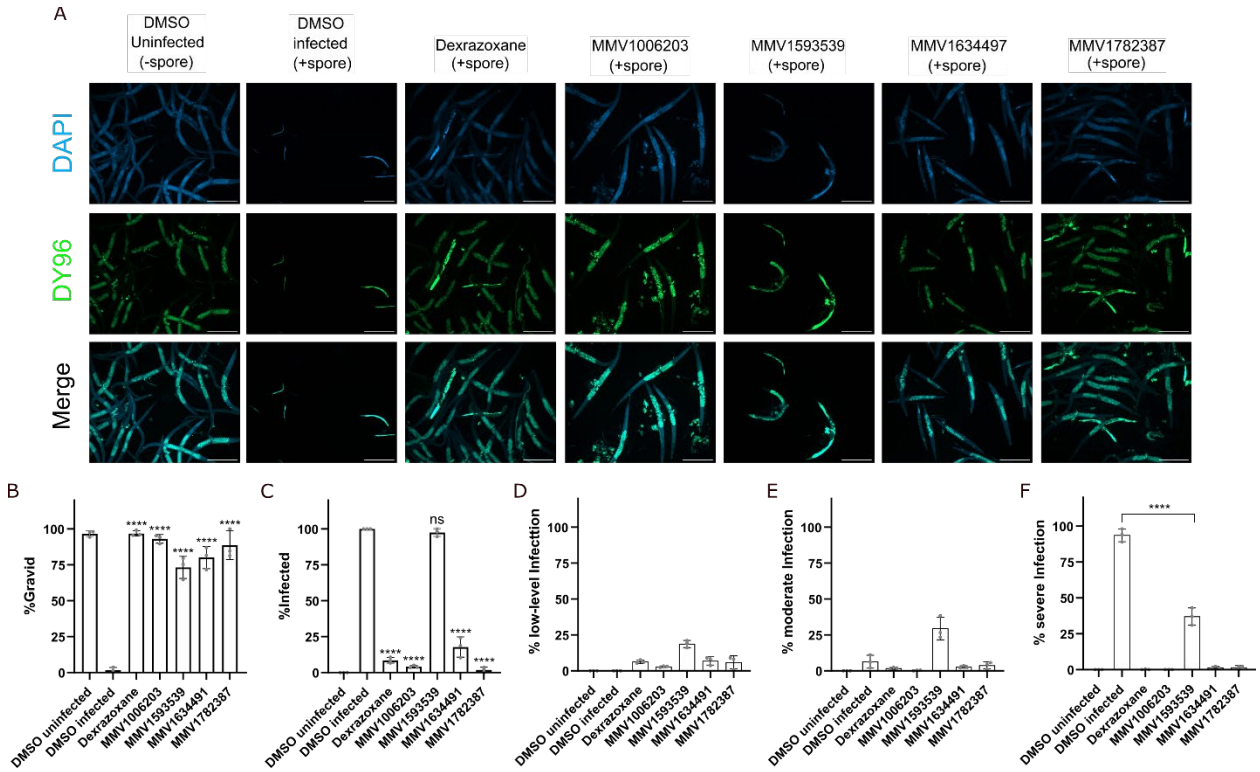

Fig. 2. Identified MMV compounds inhibit *N. parisii*. A-F L1 stage animals with incubated in the presence of *N. parisii* spores and compounds for 4 days. Animals were then fixed and stained with DY96 and DAPI. Microsporidian spores and nematode embryos are stained green by DY96. **A** Representative images of continuous infection assays taken at a magnification of 50x; scale bars are 500 µm. (First and second columns) Worms incubated without (-spore) or with spores (+spore). As a result of microsporidia infection, fewer worms become gravid, and new spores are formed. Microsporidia spores and nematode embryos are stained green by DY96. (Third to Seventh column) Dexrazoxane and the identified PRB compounds inhibit spore formation and restore embryo production. **B** The percentage of worms with embryos (n = 3, N = ≥ 100 worms counted per biological replicate). **C** The percentage of worms with newly formed spores (n = 3, N = ≥ 100 worms counted per biological replicate). **D-F** The percentage of worms with (D) low-level infection, (E) moderate infection, and (F) severe infection. The P values were determined by one-way ANOVA with post hoc test. Means ± SD (horizontal bars) are shown. (***$p < 0.001$, ****$p < 0.0001$, ns means not significant).

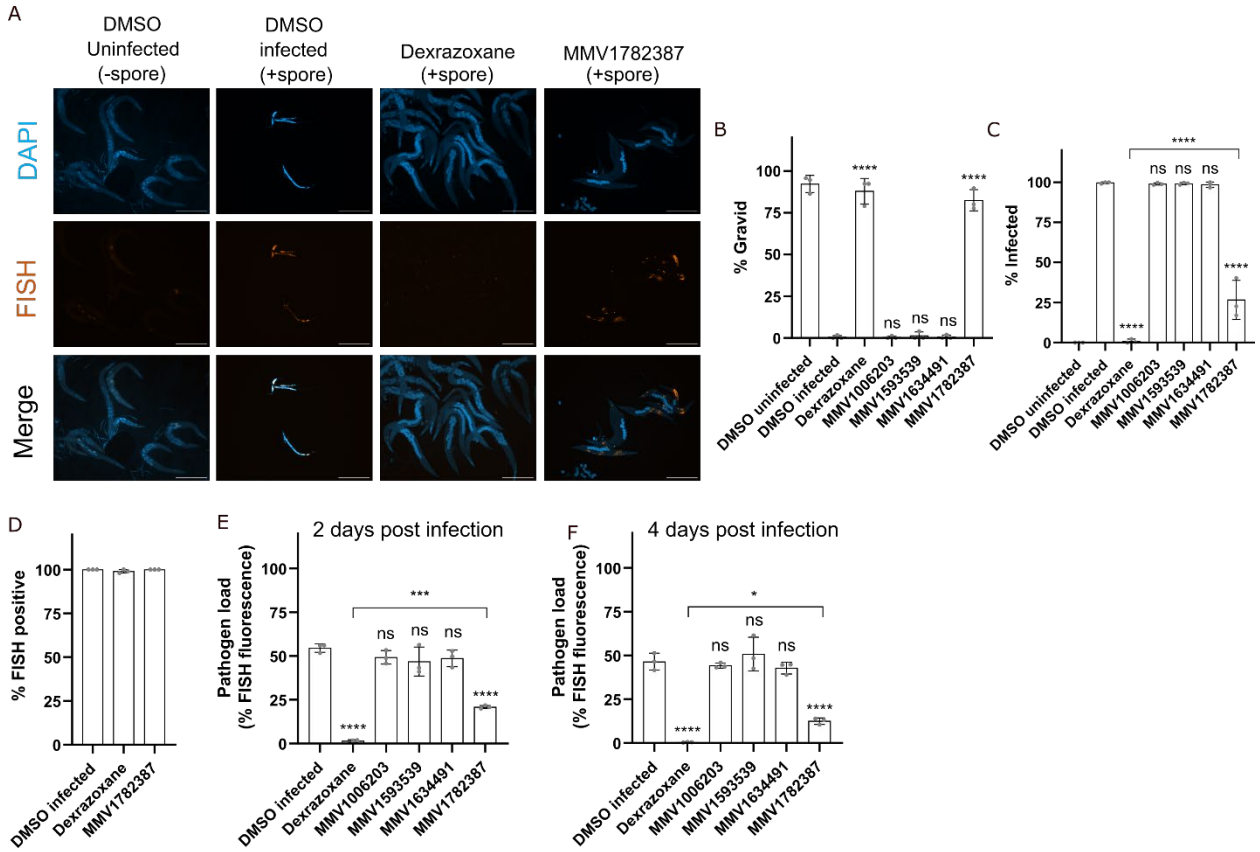

Fig.3. MMV1782387 inhibits microsporidia proliferation. A-F L1 stage animals were incubated in the presence of *N. parisii* spores for 3 hours and then washed to remove excess spores. Compounds were then added and animals were incubated for 2 (E) or 4 (A-D, F) days, fixed, and stained with DY96, DAPI and a FISH probe specific to the *N. parisii* 18S rRNA. **A** Representative images of pulse infection assays taken at a magnification of 50x; scale bars are 500 µm. (First and second columns) Worms uninfected or infected with *N. parisii* spores. Sporoplasms and meronts are stained in red with FISH probes. (Third and fourth column) Dexrazoxane or MMV1782387 treatment reduces *N. parisii* meronts. **B** The percentage of worms with embryos (n = 3, N = ≥ 100 worms counted per biological replicate). **C** The percentage of worms with newly formed spores (n = 3, N = ≥ 100 worms counted per biological replicate). **D** The percentage of worms with FISH signal (n = 3, N = ≥ 100 worms counted per biological replicate). **E, F** Quantitation of pathogen load (FISH fluorescence area %) per worm for (E) 2 or (F) 4 days post infection (n = 3, N = 10 animals quantified per biological replicate). The P values were determined by one-way ANOVA with post hoc test. Means ± SD (horizontal bars) are shown. (*p <0.05, ***p < 0.001, ****p < 0.0001, ns means not significant).

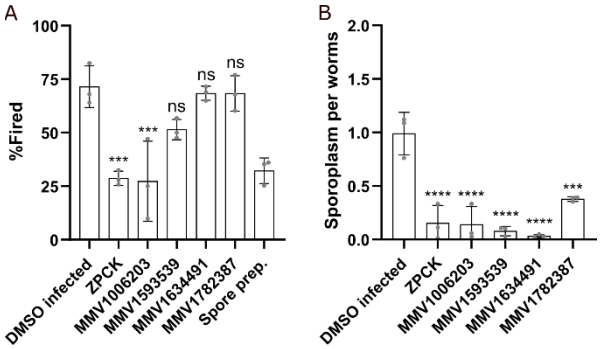

Fig.4. MMV1006203 prevent microsporidia infection by inhibiting spore firing. A, B *N. parisii* spores were incubated with compounds for 24 hours and then washed to remove compounds. Spores were then incubated with L1 stage worms for 3 hours, fixed, and stained with DY96 and *N. parisii* 18S rRNA FISH probe. **A** The percentage of fired spores in the intestinal lumen (n = 3, N = ≥ 50 spores counted per biological replicate). **B** The mean number of sporoplasms per worm (n = 3, N = ≥ 50 worms counted per biological replicate The P values were determined by one-way ANOVA with post hoc test. Means ± SD (horizontal bars) are shown. (***p < 0.001, ****p < 0.0001, ns means not significant).

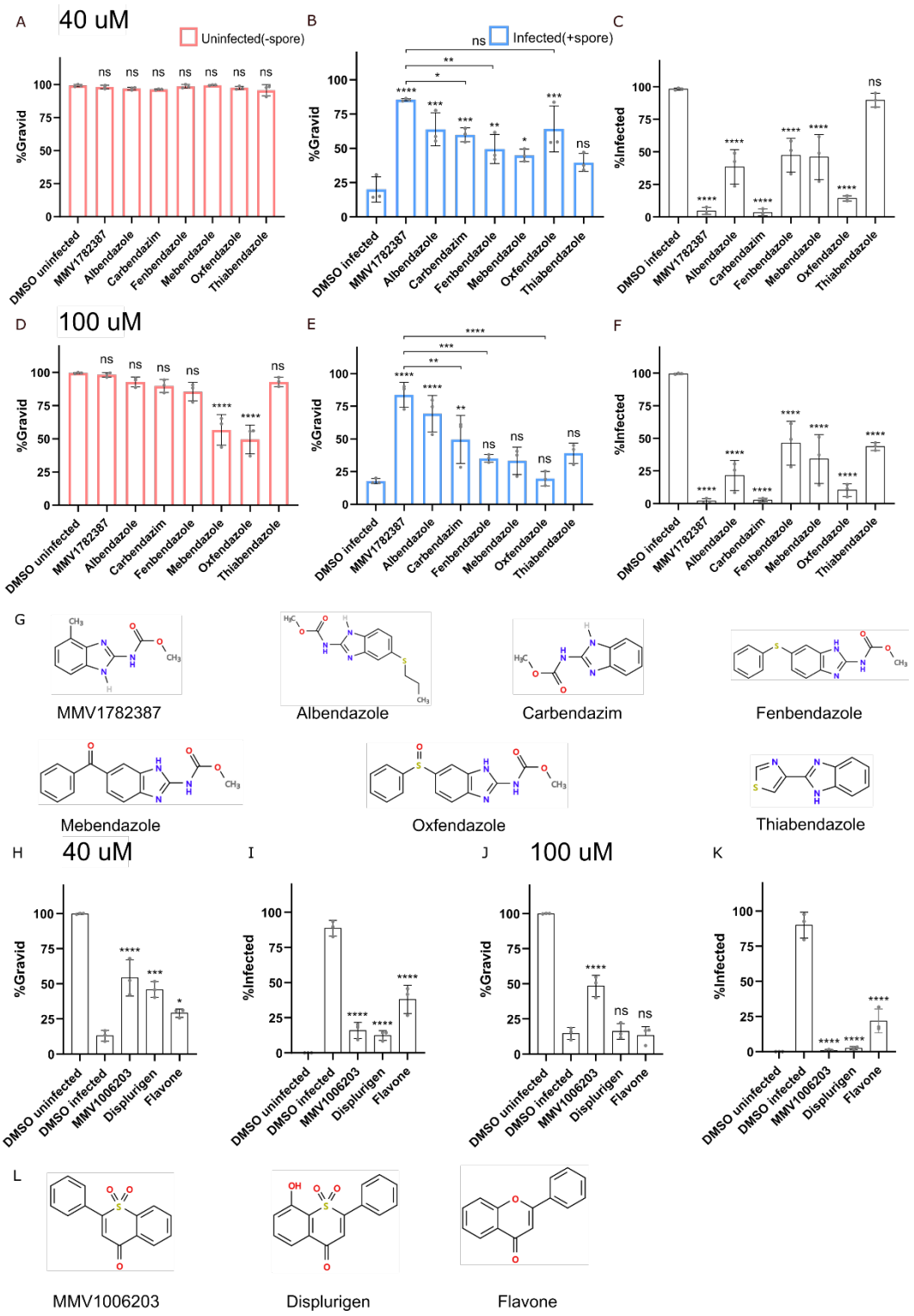

Fig.5. Benzimidazole and flavone analogs limit *N. parisii* infection. A-F, H-K L1 stage animals were continuously incubated with *N. parisii* spores and indicated compounds for 4 days, fixed, and stained with DY96 and DAPI. **A-F** Effect of benzimidazoles at 40 μM (A-C) or 100 μM

458 (D-F) on the percentage of worms with embryos in (A, D) uninfected, (B, E) infected worms and
459 (C, F) the percentage of worms with newly formed spores (n = 3, N = ≥ 100 worms counted per
460 biological replicate). **G** Chemical structures of benzimidazole analogs. **H-K** Effect of flavones at
461 40 µM (H-I) or 100 µM (J-K) on the percentage of worms with embryos (H, J) and the
462 percentage of worms with newly formed spores (I, K) (n = 3, N = ≥ 100 worms counted per
463 biological replicate). **L** Chemical structures of flavone analogs. The P values were determined
464 by one-way ANOVA with post hoc test. Means ± SD (horizontal bars) are shown. (*p < 0.05,
465 **p < 0.01, ***p < 0.001, ****p < 0.0001, ns means not significant).

466

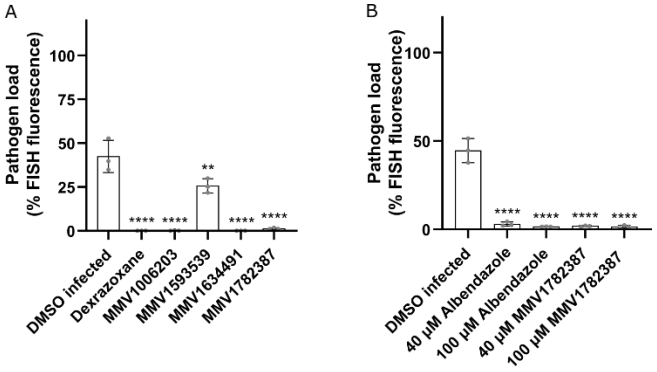

467

468 **Fig. 6. *P. epiphaga* infection is impeded by the identified inhibitors. A,B** L1 stage animals
469 were continuously incubated with *P. epiphaga* spores for four days, fixed, and stained with a *P.*
470 *epiphaga* 18S rRNA FISH probe. Quantification of pathogen load (%FISH fluorescence area) per
471 worm 4 days post infection (n = 3, N = 10 animals quantified per biological replicate). The P values
472 were determined by one-way ANOVA with post hoc test. Means ± SD (horizontal bars) are shown.
473 (*p < 0.05, **p < 0.01, ***p < 0.001).

474

475 **References**

476 AKIYOSHI D E, WEISS L M, FENG X, et al. 2007. Analysis of the β-Tubulin Genes from Enterocytozoon
477 bieneusi Isolates from a Human and Rhesus Macaque. 54: 38-41.
478 ARMSTRONG E J J O I P 1976. Fumidil B and benomyl: chemical control of Nosema kingi in Drosophila
479 willistoni. 27: 363-366.
480 BALLA K M, ANDERSEN E C, KRUGLYAK L, et al. 2015. A wild C. elegans strain has enhanced epithelial
481 immunity to a natural microsporidian parasite. 11: e1004583.
482 BALLA K M, LUALLEN R J, BAKOWSKI M A, et al. 2016. Cell-to-cell spread of microsporidia causes
483 Caenorhabditis elegans organs to form syncytia. 1: 1-6.
484 BARNES T B, VERLANGIERI A J, WILSON M C J T 1983. Reproductive toxicity of methyl-1-
485 (butylcarbamoyl)-2-benzimidazole carbamate (benomyl) in male Wistar rats. 28: 103-115.
486 BHAT I, BUHROO Z, BHAT M J I J E R 2017. Microsporidiosis in silkworms with particular reference to
487 mulberry silkworm (Bombyx Mori L.). 2: 1-9.
488 BOJKO J, REINKE A W, STENTIFORD G D, et al. 2022. Microsporidia: a new taxonomic, evolutionary, and
489 ecological synthesis.
490 BROOKS W, CRANFORD J, PEARCE L J J O I P 1978. Benomyl: effectiveness against the microsporidian
491 Nosema heliothidis in the corn earworm, Heliothis zea. 31: 239-245.
492 CHAIJARASPHONG T, MUNKONGWONGSIRI N, STENTIFORD G D, et al. 2021. The shrimp microsporidian
493 Enterocytozoon hepatopenaei (EHP): Biology, pathology, diagnostics and control. 186: 107458.
494 DANG X, PAN G, LI T, et al. 2013. Characterization of a subtilisin-like protease with apical localization
495 from microsporidian Nosema bombycis. 112: 166-174.
496 DHANAK D, KEENAN R M, BURTON G, et al. 1998. Benzothiopyran-4-one based reversible inhibitors of
497 the human cytomegalovirus (HCMV) protease. 8: 3677-3682.
498 DIDIER E S, KHAN I A J M P O O 2014. The immunology of microsporidiosis in mammals. 307-325.
499 DIDIER E S J A T 2005. Microsporidiosis: an emerging and opportunistic infection in humans and animals.
500 94: 61-76.
501 EL JARKASS H T, MOK C, SCHERTZBERG M R, et al. 2022. An intestinally secreted host factor promotes
502 microsporidia invasion of C. elegans. 11: e72458.
503 FORSGREN E, FRIES I J V P 2010. Comparative virulence of Nosema ceranae and Nosema apis in
504 individual European honey bees. 170: 212-217.
505 FRANZEN C, SALZBERGER B J A A, CHEMOTHERAPY 2008. Analysis of the β-tubulin gene from Vittaforma
506 corneae suggests benzimidazole resistance. 52: 790-793.
507 FRIES I, FENG F, DA SILVA A, et al. 1996. Nosema ceranae n. sp.(Microspora, Nosematidae),
508 morphological and molecular characterization of a microsporidian parasite of the Asian honey
509 bee Apis cerana (Hymenoptera, Apidae). 32: 356-365.
510 GUMBO T, SARBAH S, GANGAIDZO I T, et al. 1999. Intestinal parasites in patients with diarrhea and
511 human immunodeficiency virus infection in Zimbabwe. 13: 819-821.
512 HAKIM A, MOR Y, TOKER I A, et al. 2018. WorMachine: machine learning-based phenotypic analysis tool
513 for worms. 16: 1-11.
514 HAN B, TAKVORIAN P M, WEISS L M J F I M 2020. Invasion of host cells by microsporidia. 11: 172.
515 HAN B, WEISS L M J E O O T T 2018. Therapeutic targets for the treatment of microsporidiosis in humans.
516 22: 903-915.
517 HIGES M, MEANA A, BARTOLOMé C, et al. 2013. N osema ceranae (Microsporidia), a controversial 21st
518 century honey bee pathogen. 5: 17-29.
519 HORTON J J P 2000. Albendazole: a review of anthelmintic efficacy and safety in humans. 121: S113-
520 S132.

521 HOSAMANI K M, SHINGALAPUR R V J A D P 2011. Synthesis of 2‐mercaptobenzimidazole derivatives as
522 potential anti‐microbial and cytotoxic agents. 344: 311-319.
523 KATIYAR S, GORDON V, MCLAUGHLIN G, et al. 1994. Antiprotozoal activities of benzimidazoles and
524 correlations with beta-tubulin sequence. 38: 2086-2090.
525 KEELING P J P P 2009. Five questions about microsporidia. 5: e1000489.
526 KOTKOVá M, SAK B, HLáSKOVá L, et al. 2017. The course of infection caused by Encephalitozoon cuniculi
527 genotype III in immunocompetent and immunodeficient mice. 182: 16-21.
528 LABANAUSKAS L, BRUKŠTUS A, GAIDELIS P, et al. 2004. Synthesis and antiinflammatory activity of some
529 new 1-acyl derivatives of 2-methylthio-5, 6-diethoxybenzimidazole. 34: 353-355.
530 LEDER K, RYAN N, SPELMAN D, et al. 1998. Microsporidial disease in HIV-infected patients: a report of 42
531 patients and review of the literature. 30: 331-338.
532 LEFKOVE B, GOVINDARAJAN B, ARBISER J L J E R O A-I T 2007. Fumagillin: an anti-infective as a parent
533 molecule for novel angiogenesis inhibitors. 5: 573-579.
534 LEWIS J A, FLEMING J T J M I C B 1995. Basic culture methods. 48: 3-29.
535 LI J, KATIYAR S K, HAMELIN A, et al. 1996. Tubulin genes from AIDS-associated microsporidia and
536 implications for phylogeny and benzimidazole sensitivity. 78: 289-295.
537 LIM W, NYUYKONGE B, EADIE K, et al. 2022. Screening the pandemic response box identified
538 benzimidazole carbamates, Olorofim and ravuconazole as promising drug candidates for the
539 treatment of eumycetoma. 16: e0010159.
540 LV Q, ZHOU B, LIAO H, et al. 2022. Proteomic profile of polar filament and polar tube from fungal
541 pathogen microsporidium Nosema bombycis provides new insights into its unique invasion
542 organelle. 263: 104617.
543 MEAD J R, MCNAIR N J F M L 2006. Antiparasitic activity of flavonoids and isoflavones against
544 Cryptosporidium parvum and Encephalitozoon intestinalis. 259: 153-157.
545 MURAREANU B M, ANTAO N V, ZHAO W, et al. 2022. High-throughput small molecule screen identifies
546 inhibitors of microsporidia invasion and proliferation in C. elegans. 13: 5653.
547 MURAREANU B M, SUKHDEO R, QU R, et al. 2021. Generation of a microsporidia species attribute
548 database and analysis of the extensive ecological and phenotypic diversity of microsporidia. 12:
549 10.1128/mbio. 01490-01421.
550 NAVARRETE-VáZQUEZ G, HIDALGO-FIGUEROA S, TORRES-PIEDRA M, et al. 2010. Synthesis, vasorelaxant
551 activity and antihypertensive effect of benzo [d] imidazole derivatives. 18: 3985-3991.
552 PICARD-SáNCHEZ A, PIAZZON M C, AHMED N H, et al. 2020. Enterospora nucleophila (Microsporidia) in
553 gilthead sea bream (Sparus aurata): Pathological effects and cellular immune response in natural
554 infections. 57: 565-576.
555 PLESHINGER J, WEIDNER E J T J O C B 1985. The microsporidian spore invasion tube. IV. Discharge
556 activation begins with pH-triggered Ca2+ influx. 100: 1834-1838.
557 POONAM, GUPTA Y, GUPTA N, et al. 2018. Multistage inhibitors of the malaria parasite: Emerging hope
558 for chemoprotection and malaria eradication. 38: 1511-1535.
559 READER J, VAN DER WATT M E, TAYLOR D, et al. 2021. Multistage and transmission-blocking targeted
560 antimalarials discovered from the open-source MMV Pandemic Response Box. 12: 269.
561 REINKE A W, BALLA K M, BENNETT E J, et al. 2017. Identification of microsporidia host-exposed proteins
562 reveals a repertoire of rapidly evolving proteins. 8: 14023.
563 RICE C A, TROTH E V, RUSSELL A C, et al. 2020. Discovery of anti-amoebic inhibitors from screening the
564 MMV pandemic response box on Balamuthia mandrillaris, Naegleria fowleri, and Acanthamoeba
565 castellanii. 9: 476.
566 RUAN Y, XU X, HE Q, et al. 2021. The largest meta-analysis on the global prevalence of microsporidia in
567 mammals, avian and water provides insights into the epidemic features of these ubiquitous
568 pathogens. 14: 1-14.

SAKR S A, SAMEI H A, SOLIMAN M J J M S 2004. Exploring hepatotoxicity of benomyl: histological and histochemical study on albino rats. 4: 77-83.

SAMBY K, BESSON D, DUTTA A, et al. 2022. The pandemic response Box— Accelerating drug discovery efforts after disease outbreaks. 8: 713-720.

SHANLEY H T, TAKI A C, BYRNE J J, et al. 2022. A high-throughput phenotypic screen of the 'Pandemic Response Box'identifies a quinoline derivative with significant anthelmintic activity. 15: 257.

SIN N, MENG L, WANG M Q, et al. 1997. The anti-angiogenic agent fumagillin covalently binds and inhibits the methionine aminopeptidase, MetAP-2. 94: 6099-6103.

SZUMOWSKI S C, BOTTS M R, POPOVICH J J, et al. 2014. The small GTPase RAB-11 directs polarized exocytosis of the intracellular pathogen *N. parisii* for fecal-oral transmission from *C. elegans*. 111: 8215-8220.

TAMIM EL JARKASS H, REINKE A W J C M 2020. The ins and outs of host‐microsporidia interactions during invasion, proliferation and exit. 22: e13247.

TROEMEL E R, FéLIX M-A, WHITEMAN N K, et al. 2008. Microsporidia are natural intracellular parasites of the nematode Caenorhabditis elegans. 6: e309.

UNDEEN A H, FRIXIONE E J T J O P 1990. The role of osmotic pressure in the germination of nosema algerae spores 1. 37: 561-567.

UNDEEN A H J J O T B 1990. A proposed mechanism for the germination of microsporidian (Protozoa: Microspora) spores. 142: 223-235.

UNION E C J O J E 2010. Commission Regulation (EU) No 37/2010 of 22 December 2009 on pharmacologically active substances and their classification regarding maximum residue limits in foodstuffs of animal origin. 15: 1-72.

VáVRA J, RONNY LARSSON J J M P O O 2014. Structure of microsporidia. 1-70.

WADI L, EL JARKASS H T, TRAN T D, et al. 2023. Genomic and phenotypic evolution of nematode-infecting microsporidia. 19: e1011510.

WADI L, REINKE A W J P P 2020. Evolution of microsporidia: An extremely successful group of eukaryotic intracellular parasites. 16: e1008276.

WANG R, LI Q, LIU F, et al. 2022. Maturation of subtilisin-like protease NbSLP1 from microsporidia Nosema bombycis. 1126.

WANG Y, LI X-C, FU G, et al. 2017. Morphology and phylogeny of Ameson portunus n. sp.(Microsporidia) infecting the swimming crab Portunus trituberculatus from China. 61: 122-136.

WEI J, FEI Z, PAN G, et al. 2022. Current therapy and therapeutic targets for microsporidiosis. 13.

WEIDNER E, BYRD W J T J O C B 1982. The microsporidian spore invasion tube. II. Role of calcium in the activation of invasion tube discharge. 93: 970-975.

WIDMER G, AKIYOSHI D E J I, GENETICS, EVOLUTION 2010. Host-specific segregation of ribosomal nucleotide sequence diversity in the microsporidian Enterocytozoon bieneusi. 10: 122-128.

WILLIS A R, EL JARKASS H T, REINKE A W J J 2022. Studying Inherited Immunity in a Caenorhabditis elegans Model of Microsporidia Infection. e63636.

WILLIS A R, REINKE A W. Factors That determine Microsporidia infection and host specificity[C]//Microsporidia: Current Advances in Biology.Springer,2022:91-114.

WILLIS A R, ZHAO W, SUKHDEO R, et al. 2021. A parental transcriptional response to microsporidia infection induces inherited immunity in offspring. 7: eabf3114.

ZHANG G, SACHSE M, PREVOST M-C, et al. 2016. A large collection of novel nematode-infecting microsporidia and their diverse interactions with Caenorhabditis elegans and other related nematodes. 12: e1006093.